

## Basement Boundary detection by Reweighted Iterative Gravity Migration in the Erlian Basin

Zhengwei Xu\*, University of Houston; Liangjun Yan, Yangtze University; Nengyi Fu, Colorado School of Mines; Jiali Ren, University of Houston; Yang Wang, University of Houston.

### SUMMARY

3D smooth gravity migration as one of the quantitatively interpretation tools provides practical and stable image of density distribution in the subsurface. However, there are limitations to this approach, such as low resolution and inaccurate information. A new fast imaging method for 3D iterative gravity migration is introduced based on a regularized conjugate gradient (RCG) method. Remarkably, with the application of a focusing stabilizer, iterative gravity migration provides a higher resolution compared to the smooth method. In the application of imaging gravity data, the results of gravity migration can be considered as an a priori model for rigorous inversion hereafter. The practical power of the migration imaging tool is validated by a synthetic model study. Finally, a case study is presented to predict the basements boundary of the sags of the Chaokewula Depression in the Erlian Basin.

### INTRODUCTION

Knowledge of the subsurface density distribution constitutes important geophysical information that can help regional geological studies and mineral and energy resource exploration. Gravity and gravity gradiometry survey have been widely used in both mining and petroleum exploration.

Currently the only widely accepted approach for quantitative interpretation of gravity data is by rigorous inversion of the data. Successfully interpreting gravity and gravity gradiometry data via 3D density model using regularized inversion has been reported in the literature (Reamer & Ferguson, 1989; Zhdanov et al., 2004; Silva & Barbosa, 2010; Vatankhah & Ardestani, 2018; Ye & Sneeuw, 2018). However, this approach of interpretation by using 3D inversion can be a complex and time-consuming task when calculating and transforming large matrices (Xu and Zhdanov, 2015). Moreover, the quality of the inversion largely depends on a priori model as constraints into the inversion framework.

To achieve a better solution for this problem, potential field migration originally was introduced in a monograph by Zhdanov (Zhdanov, 2002). The concept of migration in geophysical fields was introduced in the context of seismic imaging (Zhdanov, 1988, 2002, 2009). It was demonstrated by Zhdanov that this concept can be applied to geopotential, such as gravity field as well. *One-step* migration potential field could be expressed by applying the adjoint operator to the observed potential data directly, resulting in fast and

stable images of properties. When making an action on the observed potential fields, *one-step* migration has been theoretically proven to be a special form of downward continuation of the potential field and/or its gradients, which is generated by the virtual image of potential sources with respect to the real observational surface into the upper half space. To get better resolution, Wan developed an algorithm using full-tensor gradient (FTG) data with a smooth stabilizer to get a higher resolution of migration image by repeating the *one-step* migration iteratively (Wan et al., 2013). Muran extended the iterative gravity migration method to joint surface and bore-hole gravity gradient data to improve the spatial resolution (Wan et al., 2016). But all the algorithms related to iterative migration mentioned above are based on steepest descent, for which convergence is relatively slow since two adjacent steepest descent directions are exactly perpendicular with each other. In other words, if we try to minimize parametric functional along direction by using steepest descent with line search, subsequent gradient directions are mutually orthogonal with each other until reach global minimum.

As another advantage of migration, any site-specific priori assumption about the source of the field is not required by the migration transformation, but is usually required in the traditional inversion method. However, a priori information can be included to reduce the uncertainty of imaging result in the framework of migration.

From dataset point of view, so far, the research related to gravity migration has been based on the complete independent gravity tensor field. Gravity gradient fields are significantly more sensitive to local anomalies than is the traditional gravity vertical field. In contrast, vertical gravity data is rarely used for gravity migration due to its low sensitivity. However, sometimes vertical gravity data is the only one which can be acquired due to limitations of instruments and conditions. In addition, the cost of acquiring vertical gravity data is relatively low, even for a large area. Therefore, it is necessary to develop an iterative gravity migration based on vertical gravity data.

In this paper, we develop an approach of using 3D iterative gravity migration of vertical gravity data based on a regularized conjugate gradient (RCG) method rather than steepest descent. To better delineate the sharp geological boundaries, we incorporate a minimum support (MS) into the algorithm by updating model weighting. We validate our new method by two model studies and a case study for 3D

## Basement Boundary detection by Reweighted Iterative Gravity Migration in the Erlian Basin

iterative gravity migration of the vertical gravity from Chaokewula Depression in the Erlian Basin.

### ADJOINT OPERATOR AND MIGRAITON FIELD

We define the vertical component of gravity field acquired on the observation surface  $S$  as  $\mathbf{g}_z^{obs}(\mathbf{r})$ , with domain  $D$  in the lower half-space, and we use  $\mathbf{A}_z^*$  as an adjoint operator for the gravity tensor field, which satisfies an explicit expression:

$$(\mathbf{A}_z(\Delta\rho_n), \mathbf{A}_z(\rho_n) - \mathbf{g}_z^{obs})_G = (\Delta\rho_n, \mathbf{A}_z^*(\mathbf{A}_z(\rho_n) - \mathbf{g}_z^{obs}))_M, \quad (1)$$

where  $\Delta\rho_n$  represents residual density at  $n$ -th iteration and  $(\mathbf{a}, \mathbf{b})$  is defined as inner product of the two vectors  $\mathbf{a}$  and  $\mathbf{b}$  in the  $L_2$  space. By taking advantage of the Euler equation and inner product in a Hilbert space, then we have adjoint operator  $\mathbf{A}_z^*$  for the gravity problem is as follows:

$$\mathbf{A}_z^*(r_n(\rho_n)) = G \iint_S \frac{r_n(\rho_n)(z-z')}{|r'-r|^3} ds, \quad (2)$$

where  $r_n(\rho_n)$  is the residual gravity field data expressed as:

$$r_n(\rho_n) = \mathbf{A}_z(\rho_n) - \mathbf{g}_z^{obs}(r). \quad (3)$$

Following Zhdanov (2002) and Zhdanov et al. (2011), an iterative migration vertical gravity field,  $\mathbf{g}_{z_n}^m(\mathbf{r})$ , is introduced as a result of application of the adjoint gravity operator,  $\mathbf{A}_z^*$ , to the residual observed vertical component of the gravity field repeatedly:

$$\mathbf{g}_{z_n}^m(\mathbf{r}) = \mathbf{A}_z^*(r_n(\rho_n)), \quad (4)$$

From a physical point of view, the iterative migration gravity field,  $\mathbf{g}_{z_n}^m(\mathbf{r})$ , is iteratively generated by the virtual image of density sources with respect to the real observational surface. Downward continuation of gravity data as a special form plays the most important role in gravity field migration. Therefore, the migration is a kind of stable transform. Furthermore, the migrated gravity field keeps remnant information of the original density distribution in the lower half-space, which illuminates the reason that it can be leveraged in imaging the sources of the gravity field.

### REWEIGHTED ITERATIVE MIGRATION

To the get a stable solution for the density distribution, we reduce the regularized inversion problem to a minimization of the parametric functional with a minimum norm stabilizer as:

$$\mathbf{P}^\alpha(\hat{\rho}^w, \mathbf{g}_z^{obs}) = \|\hat{\mathbf{A}}_z(\hat{\rho}) - \mathbf{g}_z^{obs}\|_D^2 + \alpha \|(\hat{\rho}^w - \hat{\rho}_{apr}^w)\|_M^2 \rightarrow \min, \quad (5)$$

where  $\hat{\mathbf{A}}_z$  is linear operators on the gravity field in logarithmic space.  $\hat{\rho}^w$  is introduced as a weighted transferred logarithmic density model to make sure the corresponding original density model  $\rho$  will always be confined within the assigned upper ( $\rho^+$ ) and lower bounds ( $\rho^-$ ).

An efficient approach (Portniaguine & Zhdanov, 1999), called re-weighted regularized conjugate gradient (RRCG), was introduced to minimize the parametric functional (Eq. 5). Along the RRCG direction  $\hat{\mathbf{i}}_w^\alpha(\hat{\rho}_n^{w_n})$  with line search, the  $n$ -th iteration of the RRCG inversion problem solution is given by the following:

$$\hat{\rho}_{n+1}^{w_n} = \hat{\rho}_n^{w_n} + \delta\hat{\rho}^{w_n} = \hat{\rho}_n^{w_n} - \hat{k}_n^\alpha \hat{\mathbf{i}}_w^\alpha(\hat{\rho}_n^{w_n}), \quad (6)$$

where the optimum re-weighted direction of RCG,  $\hat{\mathbf{i}}_w^\alpha(\hat{\rho}_n^{w_n})$ , satisfies a linear combination of the regularized steepest ascent  $\hat{\mathbf{i}}_w^\alpha(\hat{\rho}_n^{w_n})$  of this step and the “direction” of ascent  $\hat{\mathbf{i}}_w^\alpha(\hat{\rho}_{n-1}^{w_{n-1}})$  of the previous step as:

$$\hat{\mathbf{i}}_w^\alpha(\hat{\rho}_n^{w_n}) = \hat{\mathbf{W}}_{me_n}^{-1} L(\hat{\rho}_n) \mathbf{g}_{z_n}^m(\mathbf{r}) + \alpha \hat{\rho}_n^{w_n}, \quad (7)$$

where  $L(\hat{\rho}_n)$  is operator in transforming model into logarithmic space as:

$$L(\hat{\rho}_n) = \frac{\rho^+ - \rho^-}{(1 + \exp(\hat{\rho}_n))^2} \exp(\hat{\rho}_n), \quad (8)$$

and  $\hat{k}_n^\alpha$  is step length of each iteration inversion determined by the linear line search:

$$\hat{k}_n^\alpha = \frac{(\hat{\mathbf{i}}_w^\alpha(\hat{\rho}_n^{w_n}))^T (\hat{\mathbf{i}}_w^\alpha(\hat{\rho}_n^{w_n}))}{(\hat{\mathbf{i}}_w^\alpha(\hat{\rho}_n^{w_n}))^T ((\hat{\mathbf{A}}_{\rho_n}^{w_n})^T (\hat{\mathbf{A}}_{\rho_n}^{w_n}) + \alpha I) (\hat{\mathbf{i}}_w^\alpha(\hat{\rho}_n^{w_n}))}, \quad (9)$$

We should note, however, that the direct migration of the observed gravity field does not produce an adequate image of the subsurface density distribution because the migration fields rapidly attenuate with the depth. In order to image the sources of the gravity fields at their correct locations, one should apply an appropriate spatial weighting operator  $\hat{\mathbf{W}}_{me_n}$  shown in Eq. (7) to the migration fields. This weighting operator is constructed based on the integrated sensitivity of the data to the density multiply by focusing stabilizer (minimum support) as:

## Basement Boundary detection by Reweighted Iterative Gravity Migration in the Erlian Basin

$$\widehat{W}_{me_n} = \text{diag} \left[ c_z \frac{1}{|z|} \right] \cdot \text{diag} \left[ \frac{1}{\sqrt{(\widehat{\rho}_{n_j} - \widehat{\rho}_{apr_j})^2 + e^2}} \right]. \quad (10)$$

### SYNTHETIC STUDY: TWO-BODIES MODEL

The model consists of two rectangular bodies with the same geological properties and size submerged in a homogeneous background but buried at different depths (Figure. 1). One of the rectangular targets is at a depth of 100 m, another is at a depth of 200 m. The dimensions of the two anomalies are 100m, 150m, and 100m along with the x, y, and z directions respectively. The offset between the two anomalies is 400 m. Both bodies have a positive anomalous density of  $0.4 \text{ g/cm}^3$ . The homogeneous background for the two anomalies has density  $0 \text{ g/cm}^3$ . The synthetic vertical component of gravity data, recorded by receivers with space 20 m separation along 51 survey lines with 20 m as well, on the surface ( $z = 0 \text{ m}$ ) for this model were generated. In total 2601 observed points are acquired. There are 6400 unknown densities in the grid with each cubic cell 50 meter in length, in which we assume the density is uniform in each cell.

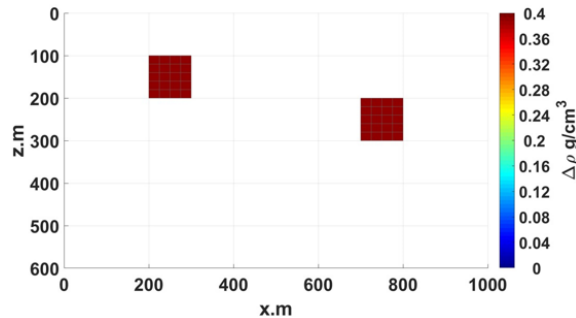


Fig. 1. The synthetic model (vertical section view)

Figure. 2 shows the vertical cross section of the migrated density distribution. The black dashed lines stand for the true position of the anomalous density bodies. It is obvious that migrated images reconstruct two anomalous bodies very well with sharp boundary. Due to applying re-weighted, even an ill-posed problem can yield a focusing image instead of smooth one.

### REAL CASE: MIGRATION OF FTG DATA AT THE ERLIAN BASIN

The study area is the Chaokewula Depression, located in the central part of the Erlian Basin (Figure. 3). The north-south oriented structure high divides the depression into

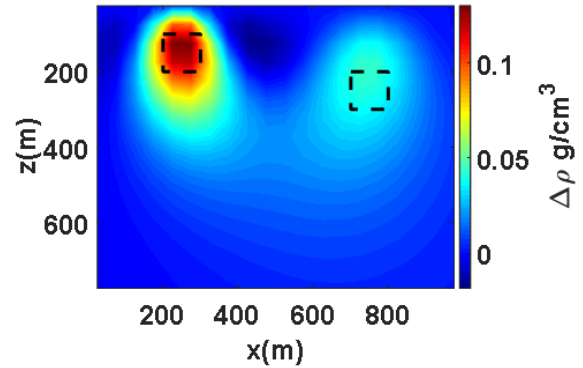


Fig. 2. The vertical section view of migrated density distribution using focusing (re-weighted) iterative gravity migration by RCG.

Eastern sag and Western sag. The basement of the basin consists of Paleozoic marine carbonates and siliciclastic interbedded with volcanic formations. The main exploration target in the basin is the Lower Cretaceous Formations and its sedimentary cover is Jurassic to Quaternary continental deposits. There are no Triassic deposits in the Chaokewula Depression. The basin evolution analysis reveals that the Chaokewula depression was a unified catchment lake basin during the deposition of Lower Cretaceous Arshan Formation and first member of the Tenge'er Formation, dominated by rifting stage conglomeratic sandstone and lacustrine mudstone. The North-South oriented structure then started to form and divide the basin into Eastern and Western sags with distinct evolutions. The second member of the Tenge'er Formation in the Eastern sag is dominated by thick deposits of shale and sandstone.

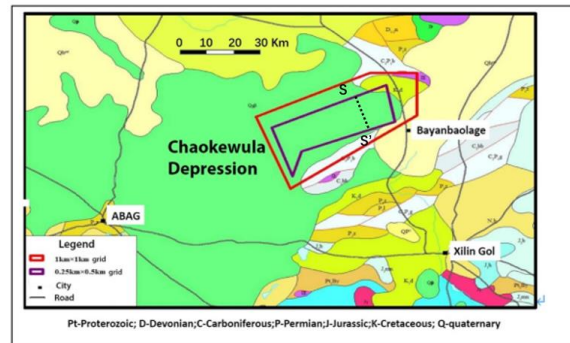


Fig. 3. The location of the Chaokewula Depression in the Erlian Basin is shown by black block, Neimenggu/Inner Mongolian Province, China. The black dash line is the 2D seismic S-S'.

The previous gravity, magnetic, magnetotelluric (MT), and seismic exploration activities in the Chaokewula Depression have not yielded good results of subsurface

## Basement Boundary detection by Reweighted Iterative Gravity Migration in the Erlian Basin

geology, which is attributed to the poor seismic imaging result due to the masking effect of volcanic rock. The key un-solved problems include the imaging of the basement of the depression, structure styles and the temporal-spatial distribution of volcanic formations in the deep intervals. We employed a high-resolution gravity survey and an integrated interpretation method to help reveal the basin architecture and stratigraphic evolution.

This paper focuses on geology, tectonics and other geological comprehensive studies in predicting the boundary of the Lower Cretaceous Formations bottom with limited seismic coverage by using  $330 \text{ km}^2$  gravity data to recover a density distribution, which was validated by the geological knowledge and one two-dimensional seismic section. So, without any prior information, gravity migration might be an appropriate interpretation tool for creating robust “big picture” of the geological structure.

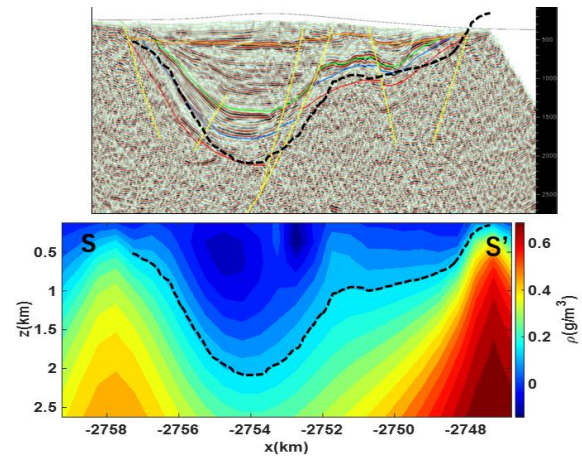
The initial model is designed as a uniform mesh model, that is, all cells are set to the same value and the model orientation is set according to the shape of the study area. The dimension of each cell is  $500\text{m} \times 500\text{m} \times 250\text{m}$ , the number of cells in the x, y, z directions is  $66 \times 26 \times 40$ , a total of 68,640 cells. The initial density field value in each cell for both prior models is  $0 \text{ g/cm}^3$ , assuming we don't have any prior information.

Figure. 4 shows the inversion result along seismic line S - S' shown in Figure 3. From the section of the migrated density, the tectonic structure of the study area can be generally recognized. It is obvious that the edge of the migrated density model of the Eastern sag correlates well with the seismic interpretation structure.

So, it is reasonable to predict basement bottom boundary by iterative gravity migration, obviating the need to collect prior information to constrain an inversion and offer a reliable tool to assist with the design of future exploration and production.

### CONCLUSIONS

Gravity field migration is a direct integral transformation of the gravity field into 3D density distributions. The derivation of iterative gravity migration is practically similar to the traditional RRCG. But the key difference between the two algorithm is that the update of the density perturbation in each iteration depends on applying the adjoint migration operator directly on the corresponding gravity residual field data. This is significant because using the powerful and



**Fig. 4. Upper panel: The seismic line S - S' in the Chaokewula Depression in the Erlian Basin. Lower Panel: the migrated density distribution along the profile S - S'. The black solid line shown in lower panel is used to delineate the boundary of basement from migrated density result.**

stable downward continuation, the iterative gravity migration makes inversion no longer the only efficient tool to get even more stable result. More importantly, the result of the migration density can be used as a reasonable prior model for robust inversion hereafter.

For synthetic study, the new approach not only predicts relatively accurate anomalous density values, but also the spatial information of the geology targets matches the models well. For the Erlian Basin real case, the result of 3D potential field iterative migration matches the geological structure interpreted by the seismic data. It may offer a robust tool to assist with the design of future seismic surveys.

### ACKNOWLEDEMENT

The study was supported by National Key R&D Program of China (2018YFC0603302) and National Natural Science Foundation of China (U1562109, 41774082).

We are thankful to the Rock Physics Lab (RPL), University of Houston for supporting this research.

## REFERENCES

- Portniaguine, O. and M. S. Zhdanov, 1999. Focusing geophysical inversion images: *Geophysics*, **64**, 874–887, doi: <https://doi.org/10.1190/1.1444596>.
- Reamer, S. K. and J. F. Ferguson, 1989. Regularized two-dimensional Fourier gravity inversion method with application to the silent canyon caldera, Nevada: *Geophysics*, **54**, 486–496, doi: <https://doi.org/10.1190/1.1442675>.
- Silva, J. B., A. S. Oliveira, and V. C. Barbosa, 2010. Gravity inversion of 2D basement relief using entropic regularization: *Geophysics*, **75**, no. 3, I29–I35, doi: <https://doi.org/10.1190/1.3374358>.
- Vatankhah, S., R. Anne Renaut, and V. E. Ardestani, 2018. A fast algorithm for regularized focused 3D inversion of gravity data using randomized singular-value decomposition: *Geophysics*, **83**, no. 4, G25–G34, doi: <https://doi.org/10.1190/geo2017-0386.1>.
- Wan, L. and M. S. Zhdanov, 2013. Iterative migration of gravity and gravity gradiometry data: 83rd Annual International Meeting, SEG, Expanded Abstracts, 1211–1215, doi: <https://doi.org/10.1190/segam2013-1036.1>.
- Wan, L., M. Han, and M. Zhdanov, 2016. Joint iterative migration of surface and borehole gravity gradiometry data: 86th Annual International Meeting, SEG, Expanded Abstracts, 1607–1611, doi: <https://doi.org/10.1190/segam2016-13849886.1>.
- Xu, Z. and M. S. Zhdanov, 2015. Three-dimensional Cole-Cole model inversion of induced polarization data based on regularized conjugate gradient method: *IEEE Geoscience and Remote Sensing Letters*, **12**, 1180–1184, doi: <https://doi.org/10.1109/LGRS.2014.2387197>.
- Ye, Z., R. Tenzer, and N. Sneeuw, 2018. Comparison of methods for a 3-D density inversion from airborne gravity gradiometry: *Studia Geophysica et Geodaetica*, **62**, 1–16, doi: <https://doi.org/10.1007/s11200-016-0492-6>.
- Zhdanov, M. S., 1988. *Integral transforms in geophysics*: Springer-Verlag.
- Zhdanov, M. S., 2002. *Geophysical inverse theory and regularization problems*: Elsevier.
- Zhdanov, M. S., R. Ellis, and S. Mukherjee, 2004. Three-dimensional regularized focusing inversion of gravity gradient tensor component data: *Geophysics*, **69**, 925–937, doi: <https://doi.org/10.1190/1.1778236>.
- Zhdanov, M. S., 2009a. *Geophysical electromagnetic theory and methods*: Elsevier.
- Zhdanov, M. S., X. Liu, G. A. Wilson, and L. Wan, 2011. Potential field migration for rapid imaging of gravity gradiometry data: *Geophysical Prospecting*, **59**, 1052–1071, doi: <https://doi.org/10.1111/j.1365-2478.2011.01005.x>.